

# Geometrical Diagnostics for Generalized Chaplygin Gas

Jianbo Lu,<sup>\*</sup> Lixin Xu<sup>†,‡</sup> Yuanxing Gui, and Baorong Chang

*School of Physics and Optoelectronic Technology,*

*Dalian University of Technology, Dalian, 116024, P. R. China*

Two geometrical diagnostic methods are applied to generalized chaplygin gas (GCG) model as the unification of dark matter and dark energy. By using the recently observed data: the Union supernovae (SNe), the observational Hubble data (OHD), the SDSS baryon acoustic peak and the five-year WMAP shift parameter, we show the discriminations between GCG and  $\Lambda$ CDM model. Furthermore, on the basis of the  $Om$  diagnostic, it can be calculated that the current equation of state (EOS) of dark energy (DE)  $w_{0de} = -0.964$  for GCG model. And for the statefinder geometrical diagnostic, it is shown that the shape of  $r(s)$  diagram much depends on the model parameter  $\alpha$ .

PACS numbers: 98.80.-k

Keywords: generalized chaplygin gas (GCG); geometrical diagnostic.

## 1. Introduction

The type Ia supernovae (SNe Ia) investigations [1], the cosmic microwave background(CMB) results from WMAP [2] observations, and surveys of galaxies [3] all suggest that the expansion of present universe is speeding up rather than slowing down. Considering that the evolution of universe complies with the four-dimensional (4D) standard cosmology, the accelerated expansion of the present universe is usually attributed to the fact that dark energy (DE) is an exotic component with negative pressure. Many kinds of DE models have already been constructed such as  $\Lambda$ CDM [4], quintessence [5], phantom [6], quintom [7], generalized Chaplygin gas (GCG) [8], modified Chaplygin gas [9], holographic dark energy [10], agegraphic dark energy[11], and so forth. Furthermore, model-independent method<sup>1</sup> and modified gravity theories (such as scalar-tensor cosmology [17], Braneworld models [18]) to interpret accelerating universe have also been discussed.

On the one hand, on the basis of cosmic observations Akaike information criterion (AIC) and Bayesian information criterion (BIC) of model selection have been used to estimate which model for an accelerating universe is distinguish by statistical analysis [19]. It can be expected that model degeneration can be avoided by the accurate observational data in the future. On the other hand, one hopes that a general and model-independent manner can be used to distinguish DE models and show the discriminations between them. Refs. [20][21] introduced two geometrical methods, i.e., statefinder diagnostic and  $Om$  diagnostic. Statefinder parameters  $\{r,s\}$  have been applied to a large number of DE

---

<sup>†</sup> Corresponding author

<sup>\*</sup>Electronic address: lvjianbo819@163.com

<sup>‡</sup>Electronic address: lxxu@dlut.edu.cn

<sup>1</sup> For example, using mathematical fundament one expands equation of state of DE  $w_{de}$  or deceleration parameter  $q$  with respect to scale factor  $a$  or redshit  $z$ , such as  $w_{de}(z) = w_0 = \text{const}$  [12],  $w_{de}(z) = w_0 + w_1 z$  [13],  $w_{de}(z) = w_0 + w_1 \ln(1+z)$  [14],  $w_{de}(z) = w_0 + \frac{w_1 z}{1+z}$  [15],  $q(z) = q_0 + q_1 z$  [12],  $q(z) = q_0 + \frac{q_1 z}{1+z}$  [16], and so forth. Where  $w_0$ ,  $w_1$ , or  $q_0$ ,  $q_1$  are model parameters.

models [20][22]. Recently,  $Om$  diagnostic is also presented in Ref. [21] to differentiate  $\Lambda$ CDM from other DE models and to understand the properties of DE. Current observations suggest an uncertainties of at least 25% in the value of current matter density  $\Omega_{0m}$  [23]. An important property for  $Om$  diagnostic is that it can be used to distinguish DE models with small influence from the density parameter  $\Omega_{0m}$ . In this paper, we apply  $Om$  and statefinder diagnostics to GCG model as the unification of dark matter and dark energy, and compare it with  $\Lambda$ CDM model.

The paper is organized as follows. In section 2, the GCG model as the unified dark sector is introduced briefly. Based on the recently observed data: the Union SNe Ia [24], the observational Hubble data (OHD) [25], the baryon acoustic oscillation (BAO) peak from Sloan Digital Sky Survey (SDSS) [26] and the five-year WMAP CMB shift parameter [27], two geometrical diagnostic approaches are applied to GCG model in section 3. Section 4 is the conclusions.

## 2. generalized Chaplygin gas model

In the GCG approach, the most interesting property is that the unknown dark sections in universe—dark energy and dark matter, can be unified by using an exotic equation of state. The energy density  $\rho$  and pressure  $p$  are related by the equation of state (EOS) [8]

$$p = -\frac{A}{\rho^\alpha}, \quad (1)$$

where  $A$  and  $\alpha$  are parameters in the model.

Considering the Friedmann-Robertson-Walker (FRW) cosmology, by using the energy conservation equation:  $d(\rho a^3) = -pd(a^3)$ , the energy density of GCG can be derived as

$$\rho_{GCG} = \rho_{0GCG} [A_s + (1 - A_s)(1 + z)^{3(1+\alpha)}]^{\frac{1}{1+\alpha}}, \quad (2)$$

where  $a$  is the scale factor,  $A_s = \frac{A}{\rho_0^{1+\alpha}}$ . For the GCG model, as a scenario of the unification of dark matter and dark energy, the GCG fluid is decomposed into two components: the dark energy component and the dark matter component, i.e.,  $\rho_{GCG} = \rho_{de} + \rho_{dm}$ ,  $p_{GCG} = p_{de}$ . Then according to the relation between the density of dark matter and redshift:

$$\rho_{dm} = \rho_{0dm}(1 + z)^3, \quad (3)$$

the energy density of the DE in the GCG model can be given by

$$\rho_{de} = \rho_{GCG} - \rho_{dm} = \rho_{0GCG} [A_s + (1 - A_s)(1 + z)^{3(1+\alpha)}]^{\frac{1}{1+\alpha}} - \rho_{0dm}(1 + z)^3. \quad (4)$$

Next, we assume the universe is filled with two components, one is the GCG component, and the other is baryon matter component, ie.,  $\rho_t = \rho_{GCG} + \rho_b$ . The equation of state of dark energy can be derived as

$$w_{de} = \frac{p_{de}}{\rho_{de}} = \frac{-(1 - \Omega_{0b})A_s[A_s + (1 - A_s)(1 + z)^{3(1+\alpha)}]^{\frac{-\alpha}{1+\alpha}}}{(1 - \Omega_{0b})[A_s + (1 - A_s)(1 + z)^{3(1+\alpha)}]^{\frac{1}{1+\alpha}} - \Omega_{0dm}(1 + z)^3}, \quad (5)$$

where  $\Omega_{0dm}$  and  $\Omega_{0b}$  are present values of the dimensionless dark matter density and baryon matter component.

In a flat universe, making use of the Friedmann equation, the Hubble parameter  $H$  can be written as

$$H^2 = \frac{8\pi G\rho_t}{3} = H_0^2 E^2, \quad (6)$$

where  $E^2 = (1 - \Omega_{0b})[A_s + (1 - A_s)(1 + z)^{3(1+\alpha)}]^{\frac{1}{1+\alpha}} + \Omega_{0b}(1 + z)^3$ .  $H_0$  denotes the present value of the Hubble parameter. Hence, the fractional energy densities of different components can be respectively expressed as

$$\Omega_{de} = \frac{(1 - \Omega_{0b})[A_s + (1 - A_s)(1 + z)^{3(1+\alpha)}]^{\frac{1}{1+\alpha}} - \Omega_{0dm}(1 + z)^3}{E^2}, \quad (7)$$

$$\Omega_{dm} = \frac{\Omega_{0dm}(1 + z)^3}{E^2}, \quad (8)$$

$$\Omega_b = \frac{\Omega_{0b}(1 + z)^3}{E^2}. \quad (9)$$

### 3. Determining $Om$ and statefinder diagnostic for GCG model from cosmic observations

#### 3.1 $Om$ diagnostic for GCG model

In order to interpret accelerating universe, many kinds of dark energy models have been constructed. They are introduced from different theories or methods, so a general and model-independent manner to distinguish these models are necessary. In what follows, we apply two geometrical approaches, i.e.,  $Om$  diagnostic and statefinder diagnostic, to the GCG model as the unification of dark matter and dark energy. And we compare the results with  $\Lambda$ CDM model to show the differences between these two models.

It is well known that model-independent quantity  $H(z)$  is important to understand the properties of DE, since its value can be directly obtained from cosmic observations (for example, the relation between luminosity distance  $D_L$  and Hubble parameter is  $H(z) = [\frac{d}{dz}(\frac{D_L(z)}{1+z})]^{-1}$  [21][28][29] for SNe investigations). Recently, a new diagnostic of dark energy  $Om$  is introduced to differentiate  $\Lambda$ CDM from other DE models. The starting point for  $Om$  diagnostic is the Hubble parameter and it is defined as [21]

$$Om(x) \equiv \frac{E^2(x) - 1}{x^3 - 1}, \quad E(x) = H(x)/H_0, \quad x = 1 + z. \quad (10)$$

For  $\Lambda$ CDM model,  $Om(z) = \Omega_{0m}$  is a constant. It provides a *null test* of cosmology constant. The benefit for  $Om$  diagnostic is that the quantity  $Om(z)$  can distinguish DE models with less dependence on matter density  $\Omega_{0m}$  relative to the EOS of DE  $w_{de}$  [21].

Next we use a combination of the recent standard candle data (307 Union SNe Ia [24]) and the OHD to constrain the evolutions of  $Om(z)$  and  $w_{de}(z)$  for GCG model with the given density parameter. The Union SNe data includes the SNe samples from the Supernova Legacy Survey (SNLS) [33], ESSENCE Surveys [34], distant SNe discovered by the Hubble Space Telescope (HST) [35], nearby SNe [36] and several other, small data sets [24]. The OHD are given by calculating the differential ages of passively evolving galaxies from the GDDS [42] and archival data [43]. Since the Hubble parameter  $H(z)$  depends on the differential age of the universe

$$H(z) = -\frac{1}{1+z} \frac{dz}{dt}, \quad (11)$$

$z$	0.09	0.17	0.27	0.40	0.88	1.30	1.43	1.53	1.75
$H(z)$ (kms $^{-1}$ Mpc) $^{-1}$	69	83	70	87	117	168	177	140	202
$1\sigma$ uncertainty	$\pm 12$	$\pm 8.3$	$\pm 14$	$\pm 17.4$	$\pm 23.4$	$\pm 13.4$	$\pm 14.2$	$\pm 14$	$\pm 40.4$

TABLE I: The observational  $H(z)$  data [25][45].

the value of  $H(z)$  can directly be measured through a determination of  $dz/dt$ . Simon *et al.* obtained nine values of  $H(z)$  in the range of  $0 < z < 1.8$  [25] (see Table I). And these nine observational Hubble data have been used to constrain several DE models [44].

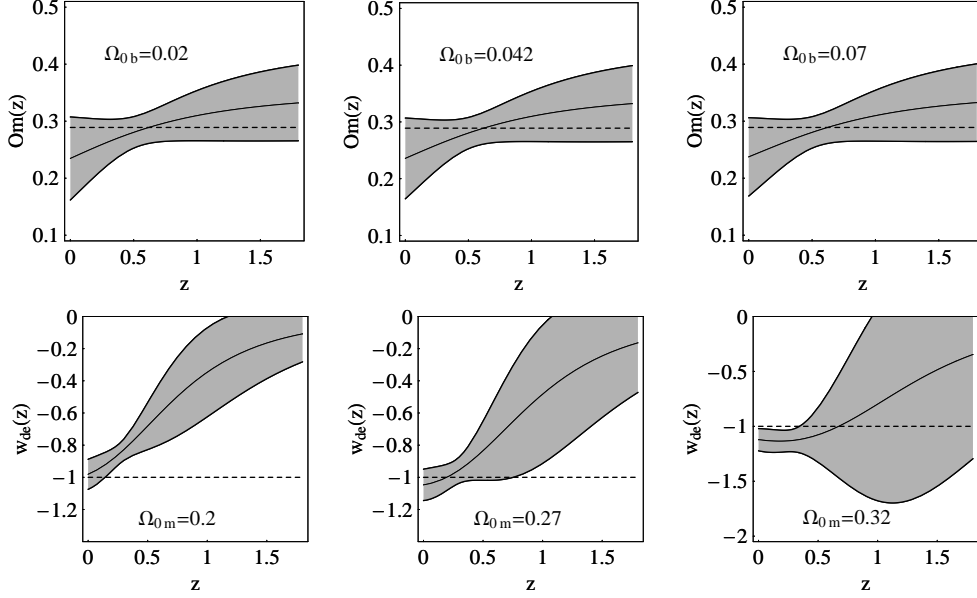


FIG. 1: Evolutions of  $Om(z)$  and  $w_{de}(z)$  from a combination of Union SNe and OHD using the GCG model. Here three different values  $\Omega_{0b}=0.02, 0.042, 0.07$  for  $Om(z)$  evolution diagram, and  $\Omega_{0m} = \Omega_{0b} + \Omega_{0dm}=0.22, 0.27, 0.32$  (i.e.,  $\Omega_{0dm}=0.2, 0.228, 0.25$ ) for  $w_{de}(z)$  diagram are assumed. The shaded regions show the  $1\sigma$  confidence level. The dashed lines show the values of  $Om(z)$  and  $w_{de}(z)$  for  $\Lambda$ CDM model.

From Eq. (5), it can be seen that both  $\Omega_{0b}$  and  $\Omega_{0dm}$  are included in the expression of  $w_{de}(z)$  for GCG model. Given three different values of  $\Omega_{0m}$ , the best fit evolutions of  $w_{de}(z)$  with  $1\sigma$  confidence level for GCG model are plotted in Fig. 1 (lower) by using the Union SNe data and the OHD. From Fig. 1 (lower), it is shown that the evolution of  $w_{de}(z)$  is sensitive to the variation of matter density  $\Omega_{0m}$ . From Eq. (6), it can be seen that the Hubble parameter  $H(z)$  for GCG model is dependent on the baryon density  $\Omega_{0b}$  and two model parameters ( $A_s, \alpha$ ). It does not explicitly include current matter density  $\Omega_{0m}$ . And we know that the observational constraints on cosmological parameter  $\Omega_{0b}$  is more stringent<sup>2</sup> relative to  $\Omega_{0m}$ , i.e., it has a relative smaller variable range [32]. on the basis of Eq. (10), we also plot the evolutions of  $Om(z)$  for GCG model in Fig. 1 by using the Union SNe data and the OHD.

<sup>2</sup> Such as  $\Omega_{0b}h^2 = 0.0214 \pm 0.0020$  from the observation of the deuterium to hydrogen ratio towards QSO absorption systems, and  $\Omega_{0b}h^2 = 0.022^{+0.004}_{-0.003}$  from the DASI results for the observation of CMB [32], here  $h = H_0/100$ .

From Fig. 1 (upper), we can see that the  $Om(z)$  diagram for GCG model as the unification of dark matter and dark energy is almost independent of the variation of  $\Omega_{0b}$ .

In Ref. [30],  $Om$  diagnostic has been used to distinguish  $\Lambda$ CDM and Ricci DE model. Assuming the matter density  $\Omega_{0m}$  to be a free parameter, Ref. [21] plots the evolution diagram of  $Om(z)$  from recently observed data by using a model-independent CPL ansatz<sup>3</sup>. In this paper, treating  $\Omega_{0b}$  as a free parameter, we apply the  $Om$  diagnostic to GCG model. One knows that for the same dark energy model, the different evolutions of cosmological quantity can be obtained from different observational datasets. This is the so-called data-dependent. And in order to diminish systematic uncertainties and get the stringent constraint on cosmological quantity, people often combine several cosmic observations to constrain the evolution of cosmological quantities. Next we use a combination of the standard candle data, the recent standard ruler data (the BAO peak from SDSS and the five-year WMAP CMB shift parameter  $R$ ) and the OHD to constrain the evolution of  $Om(z)$  for GCG model.

Because the universe has a fraction of baryons, the acoustic oscillations in the relativistic plasma would be imprinted onto the late-time power spectrum of the non-relativistic matter [37]. Therefore, the acoustic signatures in the large-scale clustering of galaxies may serve as a test to constrain models of DE with detection of a peak in the correlation function of luminous red galaxies in the SDSS [26]. The measured data at  $z_{BAO} = 0.35$  from SDSS is

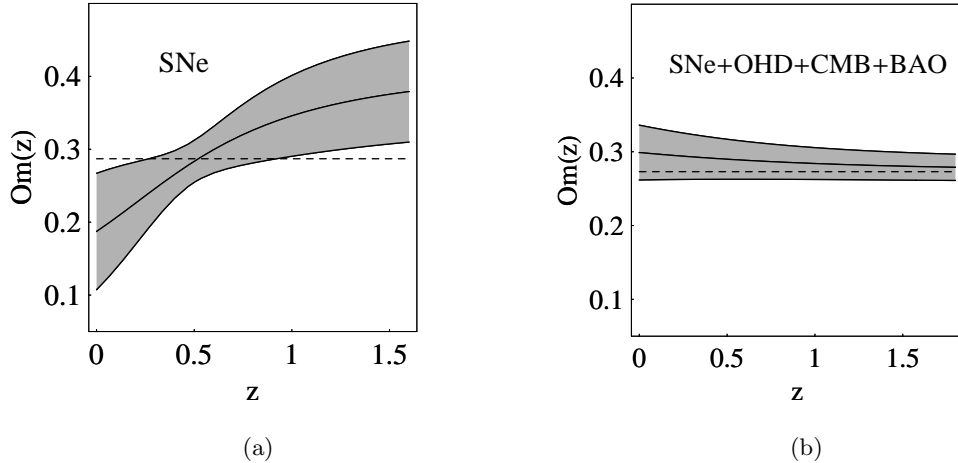
$$A = \sqrt{\Omega_{0m}^{eff}} E(z_{BAO})^{-1/3} \left[ \frac{1}{z_{BAO}} \int_0^z \frac{dz'}{E(z')} \right]^{2/3} = 0.469 \pm 0.017, \quad (12)$$

where  $\Omega_{0m}^{eff}$  is the effective matter density parameter [38][39][40].

The structure of the anisotropies of the cosmic microwave background radiation depends on two eras in cosmology, i.e., the last scattering ear and today. They can also be applied to limit DE models by using the shift parameter [41]

$$R = \sqrt{\Omega_{0m}^{eff}} \int_0^{z_{rec}} \frac{H_0 dz'}{H(z')} = 1.715 \pm 0.021, \quad (13)$$

where  $z_{rec} = 1089$  is the redshift of recombination, and the value of  $R$  is given by five-year WMAP data [27][21].




---

<sup>3</sup> It is an expansion for EOS of DE relative to scale factor  $a$ ,  $w_{de}(a) = w_0 + w_1(1 - a)$ , or  $w_{de}(z) = w_0 + \frac{w_1 z}{1+z}$  [15][31].

FIG. 2:  $Om(z)$  diagnostic for GCG model from Union SNe data and a combination of Union SNe, OHD, CMB and BAO data. Here  $\Omega_{0b}$  is treated as a free parameter. The shaded regions show the  $1\sigma$  confidence level. The dashed lines show the values of  $Om(z)$  for  $\Lambda$ CDM model obtained from the corresponding observational constraint.

On the basis of the above four observational datasets, we plot the evolution of  $Om(z)$  for GCG model in Fig. 2 (b). Here  $\chi^2_{min} = 322.411$ , and the reduced  $\chi^2$  value can be calculated by  $\chi^2_{min}/\text{dof}=1.030$ . The number of degrees of freedom (dof) for GCG model is 313 (the value of dof of the model equals the number of observational data points minus the number of parameters). And for  $\Lambda$ CDM model, the reduced  $\chi^2$  value is  $324.425/315=1.030$ , too. It shows that these two models provide an equal fit to the observational datasets. In Fig. 2, we also plot the evolution of  $Om(z)$  for GCG by using the 307 Union SNe Ia data. From Fig. 2 (a), it can be seen that the difference between GCG and  $\Lambda$ CDM model is obvious. But according to Fig. 2 (b), we can see that the best fit evolution of  $Om(z)$  for GCG model is near to  $\Lambda$ CDM case. Furthermore, we can get  $Om(0) \equiv Om(z=0) = 0.299^{+0.037}_{-0.037}$  ( $1\sigma$ ) for GCG model. And by using the above four datasets to  $\Lambda$ CDM model, it is shown that the best fit value of  $\Omega_{0m}$  and its confidence level are  $\Omega_{0m} = 0.273^{+0.016}_{-0.015}$  ( $1\sigma$ ). We know  $Om(z) = \Omega_{0m}$  for  $\Lambda$ CDM, then its best fit evolution of  $Om(z)$  is in the  $1\sigma$  confidence level of  $Om(z)$  for GCG model. And it can be seen that at  $1\sigma$  confidence level, these two models can not be clearly distinguished by current observed data according to the  $Om(z)$  diagram.

At last, according to the expression  $\frac{Om(z)-\Omega_{0m}}{1-\Omega_{0m}} \simeq 1 + w_{0de}$  ( $z \ll 1$ ) [21], it can be found that the current EOS of DE  $w_{0de} \simeq -0.964$  when take  $\Omega_{0m} = 0.273$  and the best fit value  $Om(0) = 0.299$ , which is near to  $\Lambda$ CDM model.

### 3.2 Constraint on GCG model parameters and statefinder diagnostic

According to document [20], another diagnostic of dark energy called statefinder is defined as follows:

$$r \equiv \frac{\ddot{a}}{aH^3}, \quad s \equiv \frac{r-1}{3(q-\frac{1}{2})}. \quad (14)$$

Next, we apply statefinder parameters  $\{r, s\}$  to GCG model. Like the  $Om(z)$  (10), statefinder parameters only depend upon the scale factor  $a$  and its derivative. So, both of them are "geometrical" diagnostics. It can be seen that the statefinder parameters  $\{r, s\}$  involve the third derivative of the scale factor  $a(t)$ , while  $Om$  depends upon its first derivative only. Trajectories in the  $r-s$  plane corresponding to different cosmological models exhibit qualitatively different behaviors. And for  $\Lambda$ CDM model,  $\{r, s\} = \{1, 0\}$  is a fixed point [20].

Furthermore, we can also derive the concrete expressions of the statefinder parameters

$$r = 1 + \frac{9}{2}w_{de}\Omega_{de}(1+w_{de}) - \frac{3}{2}\Omega_{de}\frac{\dot{w}_{de}}{H}, \quad s = 1 + w_{de} - \frac{\dot{w}_{de}}{3w_{de}H}. \quad (15)$$

Here  $w_{de}$  and  $\Omega_{de}$  are given by Eqs. (5) and (7) for GCG model, respectively.

By using the latest observational data: the Union SNe Ia, the observational Hubble data, the SDSS baryon acoustic peak and the five-year WMAP to GCG model, the 68.3% and 95.4% confidence level contours for model parameters  $(A_s, \alpha)$  are plotted in Fig. 3 (a). From Fig. (3) (a), we can see that the best fit values of model parameters and their confidence levels are  $A_s = 0.731^{+0.053}_{-0.059}$  ( $1\sigma$ )  $^{+0.090}_{-0.097}$  ( $2\sigma$ ),  $\alpha = -0.077^{+0.155}_{-0.126}$  ( $1\sigma$ )  $^{+0.277}_{-0.196}$  ( $2\sigma$ ). It can be seen that this constraint on parameter  $\alpha$  is more stringent than the results from Refs. [39][40], where the results of constraint on GCG model parameters are  $A_s = 0.70^{+0.16}_{-0.17}$  and  $\alpha = -0.09^{+0.54}_{-0.33}$  at  $2\sigma$  confidence level by using the X-ray gas mass fractions of galaxy clusters, the dimensionless coordinate distance of SNe Ia and FR IIb radio galaxies [39], and

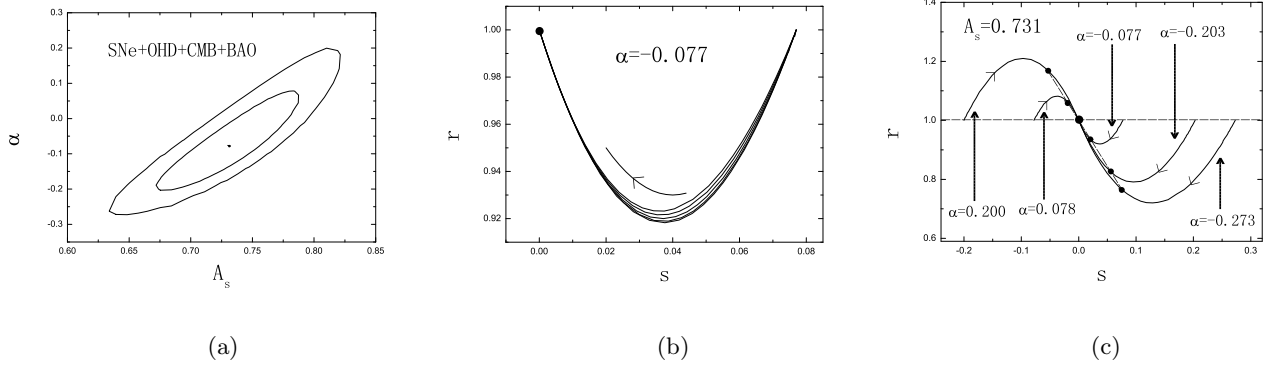


FIG. 3: The 68.3% and 95.4% confidence level contours for GCG model parameter  $A_s$  versus  $\alpha$  (a), and statefinder diagnostic for GCG model (b), (c). Here according to the combined constraint, the best fit value  $\alpha = -0.077$  is given, and  $A_s$  is setted as (0.634, 0.672, 0.731, 0.784, 0.821), respectively in (b); the best fit value  $A_s = 0.731$  is given, and  $\alpha$  is setted as (-0.273, -0.203 -0.077, 0.078, 0.200), respectively in (c). Furthermore, in figures (b) and (c) the bigger dots locate the  $\Lambda$ CDM fixed point (1,0), the smaller dots locate the current values of the statefinder pair  $\{r, s\}$ , and arrows denote the evolution directions of the statefinder trajectories  $r(s)$ .

$A_s = 0.75^{+0.08}_{-0.08}$ ,  $\alpha = 0.05^{+0.37}_{-0.26}$  at  $2\sigma$  confidence level from the nine observational Hubble data, the 115 SNLS SNe Ia data and the SDSS baryonic acoustic oscillations peak [40].

Next according to the constraint results of model parameter  $(A_s, \alpha)$  in Fig. 3 (a), we use the statefinder geometrical diagnostic to discriminate the GCG and  $\Lambda$ CDM model. From  $r$ - $s$  planes (Fig. 3 (b) and (c)), it can be found that the difference for these two model is obvious. For Fig. 3 (b), according to the combined constraint, the best fit value  $\alpha = -0.077$  is fixed and  $A_s$  is setted by the best fit value and critical values at  $1\sigma$  and  $2\sigma$  confidence level (0.634, 0.672, 0.731, 0.784, 0.821), respectively. From Fig. 3 (b), it can be seen that  $r(s)$  evolution diagram is not sensitive to the variation of value of model parameter  $A_s$ . For Fig. 3 (c), the best fit value  $A_s = 0.731$  is fixed, and  $\alpha$  is setted as (-0.273, -0.203 -0.077, 0.078, 0.200) from the constraint result, respectively. And it is obvious that the shape of  $r(s)$  diagram for this case much depends on the value of model parameter  $\alpha$ . Especially, it can be calculated that when  $\alpha = 0$ , one gets  $r = 1$ ,  $s = 0$  (here virtual number is setted as sixteen). Thus, for Fig. 3 (c) it can be divided to two regions according to the value of parameter  $\alpha$ : when  $\alpha > 0$ , one gets  $r > 1$ ,  $s < 0$ ; when  $\alpha < 0$ , one gets  $r < 1$ ,  $s > 0$ . However, when  $z$  tends to -1, no matter what value of  $\alpha$  is, we have  $\{r, s\} \simeq \{1, 0\}$ , i.e., GCG model tends to  $\Lambda$ CDM model in the distant future. Furthermore, we can see that the larger value of  $\alpha$  we have, the larger peak value is for  $r$ . And from Fig. 3 (c), it is shown that the present statefinder points,  $\{r_0, s_0\}$ , locate on a straight line. This is because when  $z = 0$ , the relationship between  $r_0$  and  $s_0$  is linear,  $r_0 = 1 + w_{0de}\Omega_{0de}s_0$ , and  $w_{0de}$ ,  $\Omega_{0de}$  are constant at this time.

#### 4. Conclusion

On the basis of the latest observational data: the Union SNe Ia data, the nine observational Hubble data, the SDSS baryon acoustic peak and the five-year WMAP, we apply two geometrical diagnostics to distinguish GCG model and  $\Lambda$ CDM model. From Fig. 1, it is shown that the larger error for the evolution of  $w_{de}(z)$  may be produced by the

erroneous estimation of matter density  $\Omega_{0m}$ . And the  $Om(z)$  is a better quantity than  $w_{de}(z)$  to truly distinguish DE models and to show the properties of DE. According to the  $Om$  diagnostic, it can be seen that for the case of the Union SNe Ia data, the difference between GCG model and  $\Lambda$ CDM model is obvious, while for the combined constraint, the best fit evolutions of  $Om(z)$  for them are similar and the difference between these two models is not clear at  $1\sigma$  confidence level. Furthermore, we also calculate the current EOS of DE,  $w_{0de} = -0.964$ , by using the value of  $Om(0)$  for GCG model. Here it should be noted that the  $Om(z)$  diagram is not sensitive to the variation of density parameter. At last, on the basis of the combined constraint, we get the best fit values and confidence levels of model parameters  $A_s = 0.731^{+0.053}_{-0.059} (1\sigma) {}^{+0.090}_{-0.097} (2\sigma)$ ,  $\alpha = -0.077^{+0.155}_{-0.126} (1\sigma) {}^{+0.277}_{-0.196} (2\sigma)$ . This constraint on parameter  $\alpha$  is more stringent than the results from Refs. [39][40]. Using the values of model parameters ( $A_s, \alpha$ ) obtained from Fig. 3 (a), we apply the statefinder parameters to discriminate the GCG and  $\Lambda$ CDM model. From r-s plane, it can be found that the difference for these two model is obvious. And it is shown that  $r(s)$  evolution diagram for GCG model much depends on the value of model parameter  $\alpha$ .

**Acknowledgments** The research work is supported by NSF (10573003), NSF (10573004), NSF (10703001), NSF (10747113), NSF (10647110), and DUT (893326) of PR China.

- 
- [1] A.G. Riess *et al*, 1998 *Astron. J.* **116** 1009 [arXiv:astro-ph/9805201]  
S. Perlmutter *et al*, 1999 *Astrophys. J.* **517** 565
  - [2] D.N. Spergel *et al*, 2003 *Astrophys. J. Suppl.* **148** 175 [arXiv:astro-ph/0302209]
  - [3] A.C. Pope *et al*, 2004 *Astrophys. J.* **607** 655 [arXiv:astro-ph/0401249]
  - [4] S. Weinberg, 1989 *Mod. Phys. Rev.* **61** 527
  - [5] B. Ratra and P.J.E. Peebles, 1988 *Phys. Rev. D.* **37** 3406
  - [6] R.R. Caldwell, M. Kamionkowski and N. N. Weinberg, 2003 *Phys. Rev. Lett.* **91** 071301 [arXiv:astro-ph/0302506]  
M.R. Setare, 2007 *Eur. Phys. J. C* **50** 991
  - [7] B. Feng, X.L. Wang and X.M. Zhang, 2005 *Phys. Lett. B* **607** 35 [arXiv:astro-ph/0404224]
  - [8] A.Y. Kamenshchik, U. Moschella and V. Pasquier, 2001 *Phys. Lett. B* **511** 265 [arXiv:gr-qc/0103004]  
P.X. Wu and H.W. Yu, 2007 *J. Cosmol. Astropart. Phys.* **0703** 015
  - [9] H.B. Benaoum, [arXiv:hep-th/0205140]  
S. Li, Y.G. Ma and Y. Chen, [arXiv:astro-ph/0809.0617]  
J.B. Lu, L.X. Xu, J.C. Li and H.Y. Liu, 2008 *Mod. Phys. Lett. A* **23** 25
  - [10] M. Li, 2004 *Phys. Lett. B* **603** 1 [arXiv:hep-th/0403127]  
Q. Wu, Y.G. Gong, A.Z. Wang and J.S. Alcanizd, 2008 *Phys. Lett. B* **659** 34  
M R Setare, 2007 *Phys.Lett.B* **648** 329 [arXiv:hep-th/0704.3679]
  - [11] R.G. Cai, 2007 *Phys. Lett. B* **657** 228 [arXiv:hep-th/0707.4049]
  - [12] A.G. Riess *et al*, 2004 *Astrophys. J.* **607** 665 [arXiv:astro-ph/0402512]
  - [13] A.R. Cooray and D. Huterer, 1999 *Astrophys. J.* **513** L95 [arXiv:astro-ph/9901097]
  - [14] B.F. Gerke and G. Efsthathiou, 2002 *Mon. Not. R. Astron. Soc.* **335** 33 [arXiv:astro-ph/0201336]
  - [15] E.V. Linder, 2003 *Phys. Rev. Lett.* **90** 091301 [arXiv:astro-ph/0208512]  
M. Chevallier and D. Polarski, 2001 *Int. J. Mod. Phys. D* **10** 213 [arXiv:gr-qc/0009008]
  - [16] L.X. Xu and J.B. Lu, accepted by *Mod. Phys. Lett. A*



- [17] B. Boisseau, G. Esposito-Farese, D. Polarski and A. A. Starobinsky, 2000 *Phys. Rev. Lett.* **85** 2236 [arXiv:gr-qc/0001066]
- [18] V. Sahni, Yu. Shtanov and A. Viznyuk, 2005 *J. Cosmol. Astropart. Phys.* **0512** 005 [arXiv:astro-ph/0505004]  
I. Brevik, 2008 *Eur. Phys. J. C* **56** 579
- [19] A.R. Liddle, 2004 *Mon. Not. R. Astron. Soc.* **351** L49 [arXiv:astro-ph/0401198]  
J.B. Lu *et al*, 2008 *Phys. Lett. B* **662**, 87  
M. Szydlowski and W. Godlowski, 2006 *Phys. Lett. B* **633** 427 [arXiv:astro-ph/0509415]
- [20] V. Sahni and T.D. Saini, A. A. Starobinsky and U. Alam, 2003 *JETP Lett.* **77** 201-206
- [21] V. Sahni, A. Shafieloo and A. A. Starobinsky, 2008 *Phys. Rev. D* **78** 103502 [arXiv:astro-ph/0807.3548]
- [22] U. Alam, V. Sahni, T. D. Saini and A. A. Starobinsky arXiv:astro-ph/0303009]  
B.R. Chang *et al*, 2007 *J. Cosmol. Astropart. Phys.* **0701** 016 [arXiv:astro-ph/0612616]
- [23] E. Komatsu *et al*, [arXiv:astro-ph/0803.0547]
- [24] D. Rubin *et al*, [arXiv:astro-ph/0807.1108]
- [25] J. Simon *et al*, 2005 *Phys. Rev. D* **71**, 123001
- [26] D.J. Eisenstein *et al*, 2005 *Astrophys. J.* **633**, 560 [arXiv:astro-ph/0501171]
- [27] J. Dunkley *et al*, [astro-ph/0803.0586]
- [28] T. Nakamura and T. Chiba, 1999 *Mon. Not. R. Astron. Soc.* **306** 696 [arXiv:astro-ph/9810447]
- [29] T.D. Saini, S. Raychaudhury, V. Sahni and A.A. Starobinsky, 2000 *Phys. Rev. Lett.* **85** 1162 [arXiv:astro-ph/9910231]
- [30] C.J. Feng, [arXiv:astro-ph/0809.2502]
- [31] E. M. Barboza Jr. and J. S. Alcaniz, 2008 *Phys. Lett. B* **666** 415-419 [arXiv:astro-ph/0805.1713]
- [32] D. Kirkman *et al*, 2003 *Astrophys. J. Suppl.* **149** 1 [arXiv:astro-ph/0302006]  
C. Pryke *et al*, 2002 *Astrophys. J.* **568** 46 astro-ph/0104490
- [33] P. Astier *et al*, 2006 *Astron. Astrophys.* **447** 31 [arXiv:astro-ph/0510447]
- [34] W.M. Wood-Vasey *et al*, [arXiv:astro-ph/0701041]
- [35] A.G. Riess *et al*, [arXiv:astro-ph/0611572]
- [36] M. Hamuy, M.M. Phillips, N.B. Suntzeff, R.A. Schommer and J. Maza, 1996 *Astron. J.* **112** 2408 [arXiv:astro-ph/9609064]  
S. Jha, A. G. Riess and R. P. Kirshner, 2007 *Astrophys. J.* **659** 122 [arXiv:astro-ph/0612666]
- [37] D.J. Eisenstein and W. Hu, 1998 *Astrophys. J.* **496** 605 [arXiv:astro-ph/9709112]
- [38] M. Makler, S.Q. Oliveira and I. Waga, 2003 *Phys. Rev. D* **68** 123521  
J.A.S. Lima, J.V. Cunha and J.S. Alcaniz, [arXiv:astro-ph/0611007]
- [39] Z.H. Zhu, 2004 *Astron. Astrophys.* **423** 421
- [40] P. Wu and H.W. Yu 2007 *Phys. Lett. B* **644** 16
- [41] J.R. Bond, G. Efstathiou and M. Tegmark, 1997 *Mon. Not. R. Astron. Soc.* **291**, L33 [arXiv:astro-ph/9702100]
- [42] R.G. Abraham *et al*, 2003 *Astron. J.* **593** 622
- [43] T. Treu *et al*, 1999 *Mon. Not. R. Astron. Soc.* **308** 1037  
T. Treu *et al*, 2001 *Mon. Not. R. Astron. Soc.* **326** 221
- [44] Z.L. Yi and T.J. Zhang, 2007 *Mod. Phys. Lett. A* **22** 41-53 [arXiv:astro-ph/0605596]  
H. Wei, S. N. Zhang, 2007 *Phys. Lett. B* **644** 7 [astro-ph/0609597]  
J.B Lu, L.X Xu, M.L Liu and Y.X Gui, 2008 *Eur. Phys. J. C* **58** 311 [arXiv:astro-ph/0812.3209]  
Hui Lin *et al*, [arXiv:astro-ph/0804.3135]
- [45] L. Samushia and B. Ratra, 2006 *Astrophys. J.* **650** L5 [astro-ph/0607301]  
R. Jimenez, L. Verde, T. Treu and D. Stern, 2003 *Astrophys. J.* **593** 622 [astro-ph/0302560]